Adaptive Large MISO Downlink with Predictor Antennas Array for very fast moving vehicles

Dinh-Thuy Phan-Huy*
*Orange Labs
dinhthuy.phanhuy@orange.com

Mikael Sternad**
**Uppsala University
mikael.Sternad@signal.uu.se

Tommy Svensson†
†Chalmers University of Technology
tommy.svensson@chalmers.se

Abstract—**Recently, a "Separate Receive and Training Antenna" technique has been proposed to provide energy efficient and robust wireless downlink data transmission towards antennas placed upon fast moving vehicles. Energy efficiency is attained thanks to Large Multiple Input Single Output Beamforming. Robustness to beamforming mispointing at high speed is obtained by using the recent "Predictor Antenna" concept. However, for some speeds, the Separate Receive and Training Antenna technique suffers from residual mispointing. To improve the robustness of this technique, we propose three new schemes: the "Border Switch Off Scheme", the "Random Switch Off Scheme" and the "Polynomial Interpolation" scheme. The two first schemes dynamically mute transmit antennas selectively when the residual mispointing is too severe. The third scheme generalizes the Predictor Antenna concept and uses all antennas upon the vehicle as a Predictor Antennas Array. These schemes are here assessed over spatially correlated channels. The two first schemes reduce energy saving to slightly improve robustness, whereas the third scheme perfectly compensates all speeds up to 300 kmph with maximum energy saving, at the cost of extra complexity.**

Keywords-component; wireless, beamforming, high velocity, moving cells, TDD, large MISO, predictor antenna.

I. INTRODUCTION

In Time Division Duplex (TDD) wireless communications, channel reciprocity and Channel State Information at the Transmitter (CSIT) can be exploited by Multiple Input Single Output (MISO) techniques, such as Maximum Ratio Transmission (MRT) Beamforming (BF) [1], to achieve a high performance, still with a low complexity [2]. Recent work has shown that very large antenna arrays at the Base Station (BS) save energy without performance degradation [2-5], and that the theoretical energy saving at the BS increases linearly with the number of uncorrelated transmit antennas [3-5].

In a conventional TDD system, which we will refer to as "Reference System" (RS), the mobile station (MS) sends pilots in the uplink (UL), the BS acquires CSIT to predict the channel, and computes BF weights. Later on, the BS transmits data in the downlink (DL) using these weights. Thanks to BF, a lower transmit power achieves the target Signal-To-Noise Ratio (SNR). Energy saving and target SNR are then both achieved for low speed MS. Unfortunately, for a fast moving MS in multipath scattering environments, the channel prediction is outdated due to short-term fading. BF mispointing then occurs due to the delay between the UL and DL phases and the target SNR and Block Error Rate (BLER) targets are not achieved. Conventional prediction is not robust to high mobility, in terms of BLER.

Recently, for the particular case of vehicular moving relays [6], [7] has introduced the new fundamental concept of "Predictor Antenna" (PA). A PA is positioned on the roof of a vehicle and one or several separate receive antennas are aligned behind the PA. The vehicle is assumed to move through a stationary electromagnetic standing wave pattern, i.e. . In other words, the BS creates a static electromagnetic field, and the vehicle simply moves through it. Due to this movement, receive antennas naturally replace the PA and see the same channel as the PA, but simply a bit later. The PA can therefore predict the channel of the receive antennas. This generic concept is an enabler for any technique based on CSIT. It is not restricted to TDD and it is applicable to DL and UL. Further analysis and experimental validation of the concept with a vehicle in outdoor urban areas has been conducted in [7-11].

Very recently, for the particular purpose of large MISO DL BF in TDD, a new scheme called Separate Receive and Training Antennas (SRTA) [13], has been proposed to achieve high energy efficient wireless downlink towards very fast moving vehicles. The vehicle roof has one PA at the front and several "Candidate Antennas" (CAs) aligned behind. The PA sends pilots in the UL and the BS computes BF weights. Among the CAs, a "Receive Antenna" (RA), responsible for data demodulation, is dynamically selected among the CAs as a function of the vehicle speed. The TDD frame is also dynamically extended. The RA is selected and the extended frame is computed to ensure that, during the DL phase, the RA is at the position that was previously occupied by the PA during the UL phase. Current standards support frame extensions with a time granularity of 1 ms [14]. However, with such a coarse granularity, SRTA performance still suffers from residual BF mispointing [13]. A somewhat similar scheme was proposed in [15]. There, antennas on the vehicle roof are transmitting successively to perform uplink beamforming from a roughly fixed position in space.

We here propose two ways to improve SRTA robustness.

- We first investigate a low complexity approach which consists in muting some transmit antennas to widen the beam when mispointing is too severe. Two schemes are studied: the "border Switch Off Scheme" (B-SOS), and the "Random Switch Off Scheme" R-SOS, namely.
- We then explore a more complex approach, through the "Polynomial Interpolation" (PI) scheme, where all antennas at the vehicle are considered as a Predictor

Antennas Array. Measurements are collected by all PAs, during multiple periods, to get a picture of the channel over a dense pattern of positions in space. As these positions surround the position for which the channel must be predicted, polynomial interpolation can be used to provide more a accurate prediction than extrapolation [7].

The paper is organized as follows. Section II presents our generic transmission model. Schemes specific parameters are detailed in section III. Section IV gives an initial analysis which is then confirmed by simulation results presented in section V. Section VI concludes the paper. The following notations are used throughout the paper: $\vec{v} \in \mathbb{R}^3$ is a vector with Cartesian coordinates; if $u \in \mathbb{R}$, $[u]$ is the integer part of u; if $u \in \mathbb{C}$, $|u|$ is its module; if $\vec{v} \in \mathbb{R}^3$, $\|\vec{v}\|$ is its norm. $[a, b[= \{x \in \mathbb{R} | a \leq t < b\}$.

II. Common System Model

This section presents common parameters and constrains for the proposed and investigated downlink transmit schemes.

We consider a DL wireless backhaul link between a BS and a vehicle moving with a velocity vector $\vec{v}$ and speed $v = \|\vec{v}\|$. All schemes use MISO MRT BF weights based on CSIT, and target the same SNR x_T. The required prediction horizon between CSIT and data transmission is at least t_0, with t_0 being the minimum time required for processing at the BS.

A. Antennas and positions at different times

The BS has K antenna(s), each with an index $k \in A_0$, with $A_0 = \{k \in \mathbb{N}, 0 \leq k < K\}$. A subset $A \subseteq A_0$ of K_a antenna(s) is active. The vehicle has L antenna(s), each with an index $l \in \Lambda$, with $\Lambda = \{l \in \mathbb{N}, 0 \leq l < L\}$. Among these antennas, one antenna called RA, is responsible for DL data demodulation, and P antenna(s), called PA(s), each with an index $l \in \Pi$, with $\Pi = \{l \in \mathbb{N}, 0 \leq l < P\}$ is(are) responsible for sending pilots in the UL. Let l_a be the RA index.

Fig. 1 Vehicle antennas

As illustrated by Fig. 1, antennas are spaced by Δ and aligned with $\vec{v}$, behind antenna $l = 0$. Let $\overrightarrow{n_l^m}$ and $\overrightarrow{n_l'}$ be the position vectors of antenna l at times τ^m and t' (to be defined later on), respectively. We assume that $\overrightarrow{n_l^m}$ and $\overrightarrow{n_l'}$ satisfy:

$$\overrightarrow{n_l'} - \overrightarrow{n_0'} = \overrightarrow{n_l^m} - \overrightarrow{n_0^m} = -l\Delta v^{-1}\vec{v}, \quad (1)$$

$$\overrightarrow{n_l'} - \overrightarrow{n_l^m} = (t' - \tau^m)\vec{v}. \quad (2)$$

The following simplified notations will be used for the two particular positions $\overrightarrow{n_0^0}$ and $\overrightarrow{n_{l_a}'}$:

$$\vec{\alpha} = \overrightarrow{n_0^0}, \quad (3)$$

$$\vec{\varepsilon} = \overrightarrow{n_{l_a}'}. \quad (4)$$

B. Static Spatially Correlated Channel Model

The vehicle is assumed to be moving in a time-invariant and spatially correlated fading propagation channel, which will be further described in section IV.A. This assumption has been verified experimentally in [7-11]. Orthogonal Frequency Division Duplex (OFDM) is assumed. Hence, for a given sub-carrier and OFDM symbol, the channel gain between BS antenna k and any antenna at position $\vec{n}$ can be modeled by a complex coefficient $g_k(\vec{n})$. Measurement-based investigations [11] have shown that a very high correlation can be obtained between the channel from/to two antennas on a vehicle that at different time instants move through the same position. In this paper, we assume that the two channels seen by two antennas successively occupying the same position in space are equal.

C. TDD frame and delay between CSIT acquisition and BF

We consider a TDD frame, with UL and DL periods $[-\tau^{UL}, 0[$ and $[0, \tau^{DL}[$, respectively. CSIT acquisition and BF are performed on a per OFDM symbol and sub-carrier basis. For every symbol, sub-carrier and antenna k, the BS measures and stores a channel coefficient and computes a BF weight. In practice, the frequency of BF coefficients updates in the time and frequency domains would be optimized according to the channel coherence time and coherence bandwidth. The following mathematical description is valid for any sub-carrier, symbol and antenna $k \in K_a$. At time $t' \in [0, \tau^{DL}[$, the BS uses pre-computed predictions $\gamma_k(\vec{\varepsilon})$ of $g_k(\vec{\varepsilon})$ to transmit data with the MRT BF [1,2] weights p_k:

$$p_k = \gamma_k^*(\vec{\varepsilon}). \quad (5)$$

We constrain the predictions to be computed based on a set of channel measurement(s) $C = \left\{\hat{g}_k\left(\overrightarrow{n_l^m}\right) \middle| m \in \Gamma, l \in \Pi\right\}$, where $\hat{g}_k\left(\overrightarrow{n_l^m}\right)$ is the measurement of $g_k\left(\overrightarrow{n_l^m}\right)$ performed by the BS using pilots received from PA l at an earlier time $\tau^m \in [-\tau^{UL}, 0[$, $\Gamma = \{m \in \mathbb{N}, 0 \leq m < M\}$ and $M \geq 1$. We also constrain the prediction horizon δ^m between t' and τ^m to satisfy:

$$\delta^m = t' - \tau^m \text{ and } \delta^m \geq t_0. \quad (6)$$

Finally, we define the number of measurement samples as $N_{meas} = card(C) \geq 1$, and assume perfect measurements:

$$\hat{g}_k\left(\overrightarrow{n_l^m}\right) = g_k\left(\overrightarrow{n_l^m}\right). \quad (7)$$

D. Performance Metrics

To save energy, the BS computes the transmit power E per unit bandwidth (based on $\gamma_k(\vec{\varepsilon})$ and p_k,) adjusted to attain a target SNR x_T. Since $x_T N_0$ is the total received power per unit bandwidth,

$$x_T = E{N_0}^{-1}|\sum_{k=1}^{K} p_k \gamma_k(\vec{\varepsilon})|^2, \quad (8)$$

where N_0 is the noise power per unit bandwidth at the receiver. The target transmit power E is obtained from (5) and (8) as

$$E = x_T N_0 |\sum_{k \in A} |\gamma_k(\vec{\varepsilon})|^2|^{-2}. \quad (9)$$

In current standards [14], the subcarrier spacing is large enough so that Inter Carrier Interference can be neglected even for high speed. Therefore, the achieved SNR x is approximately:

$$x = E{N_0}^{-1}|\sum_{k=1}^{K} g_k(\vec{\varepsilon}) p_k|^2. \quad (10)$$

By inserting (5) and (9) into (10), one obtains:

$$x = x_T |\sum_{k\in A} g_k(\vec{\varepsilon}) \gamma_k^*(\vec{\varepsilon})|^2 |\sum_{k\in A} |\gamma_k(\vec{\varepsilon})|^2|^{-2}. \quad (11)$$

The energy saving due to MISO BF is defined as $e_S = E_1/E$, where $E_1 = x_T N_0 (|p_0|^2)^{-2} = x_T N_0 |p_0|^{-4}$ is the energy required with $K_a = 1$ antenna. Hence, the expression of e_S is given by:

$$e_S = |\sum_{k\in A} |\gamma_k(\vec{\varepsilon})/\gamma_0(\vec{\varepsilon})|^2|^2. \quad (12)$$

Note that x and e_S depend on $\gamma_k(\vec{\varepsilon})$ and $g_k(\vec{\varepsilon})$ only. If the prediction is accurate (i.e. $\gamma_k(\vec{\varepsilon}) = g_k(\vec{\varepsilon})$), then (9) reduces to $x = x_T$, i.e. the SNR target is met. Otherwise, BF mispointing occurs.

III. Specific System Models

The investigated schemes differ by the values of the parameters K_a, A_0, M, P, L, τ^{UL}, τ^{DL}, δ^m, and l_a previously introduced in Section II, the prediction $\gamma_k(\vec{\varepsilon})$ and the resulting performance metrics x and e_S.

A. Reference System (RS)

For RS, all antennas at the BS side are used. At the vehicle side, a single antenna is used both for prediction and data reception. The UL/DL frames are set equal to the smallest value (i.e. t_0) to minimize the mispointing. A single measurement from the PA is used for prediction, with a processing delay equal to the frame duration. More precisely, $K_a = K$, $A = A_0$, $M = P = L = 1$, $\tau^{DL} = \tau^{UL} = \delta^0 = t_0$ and $l_a = 0$. With these assumptions and (7), we use a simple extrapolation in time of the present channel estimate as channel predictor.

$$\gamma_k(\vec{\varepsilon}) = g_k(\vec{\alpha}), \quad (13)$$

The SNR x and the energy saving ratio e_S are then derived using (1)-(6) and (10)-(12):

$$x = \frac{|\sum_{k\in A_0} g_k(\vec{\alpha}+t_0\vec{v}) g_k^*(\vec{\alpha})|^2}{|\sum_{k\in A_0} |g_k(\vec{\alpha})|^2|^2} x_T. \quad (14)$$

$$e_S = |\sum_{k\in A_0} |g_k(\vec{\alpha})/g_0(\vec{\alpha})|^2|^2. \quad (15)$$

One can notice that x is speed-dependent whereas e_S is constant. At low speed, the SNR is met whereas at high speed, mispointing occurs and we expect SNR to be lower than x_T.

B. Separate Receive and Training Antennas (SRTA)

This section briefly recalls the SRTA [13] scheme. As for RS, all transmit antennas are used, and the UL/DL frames are equal. Prediction relies on a single measurement from a single PA, with a processing delay equal to the frame duration. The BS and the vehicle are assumed to have a perfect estimate of the speed using e.g. the Global Positioning System (GPS).

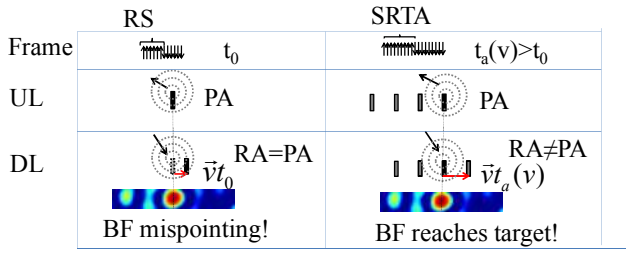

Fig. 2 RS and SRTA systems

As illustrated in Fig. 2, SRTA avoids mispointing by selecting dynamically, and according to speed, an extended frame and the RA is selected among several CAs located behind the PA, to ensure that the RA is at the previous position of the PA. More precisely, $K_a = K$, $A = A_0$, $M = P = 1$, $L > 1$, $\tau^{DL} = \tau^{UL} = \delta^0 = t_a(v) > t_0$ and $l_a = r_a(v)$. The PA has index $l = 0$. The vehicle signals to the BS. The RA antenna index $r_a(v)$ and $t_a(v)$, which defines the frame duration and the prediction horizon, are then selected to ensure that $\vec{\varepsilon} \approx \vec{\alpha}$. In current standards [14], frames are adaptive by steps of d. Reference [13] suggests the following choices of $r_a(v)$, $t_a(v)$ and $\vec{\varepsilon}$ as functions of d:

$$r_a(v) = min\{\, l \in \Lambda \mid [l\Delta(dv)^{-1}]d > t_0 \,\}, \quad (16)$$

$$t_a(v) = [r_a(v)\Delta v^{-1} d^{-1}]d, \quad (17)$$

$$\rho(v) = [r_a(v)\Delta(dv)^{-1}]dv - r_a(v)\Delta. \quad (18)$$

$$\vec{\varepsilon} = \vec{\alpha} + \rho(v) v^{-1} \vec{v}, \quad (19)$$

The relation (17) above ensures that (13) is attained for speeds up to v_{max}, given by $v_{max} = (L-1)\Delta|t_0|^{-1}$. The prediction in this case is, as for RS: $\gamma_k(\vec{\varepsilon}) = g_k(\vec{\alpha})$. Finally, x and e_S are derived in [13] as follows:

$$x = \frac{|\sum_{k\in A_0} g_k(\vec{\alpha}+\rho(v)v^{-1}\vec{v}) g_k^*(\vec{\alpha})|^2}{|\sum_{k\in A_0} |g_k(\vec{\alpha})|^2|^2} x_T. \quad (20)$$

$$e_S = |\sum_{k\in A_0} |g_k(\vec{\alpha})/g_0(\vec{\alpha})|^2|^2. \quad (21)$$

As for RS, x is speed dependent and e_S is constant. For $v \in V$, (with $V = \{u = \Delta(dp)^{-1} | p \in [\![1, L-1]\!]\}$) $x = x_T$, whereas for $v \notin V$, due to the granularity d (see [13]), $x \neq x_T$. In other words, $v \in V$ is a "perfectly compensated" (PC) speed and $v \notin V$ is a "non perfectly compensated" (NPC) speed.

C. SRTA with Switch Off Scheme (SOS)

SOS is used on top of SRTA, to reduce the SNR and BLER degradation due to residual BF mispointing for NPC speeds identified in section III.B. SOS detects mispointing and widens the beam, by switching off BS antennas.

As illustrated in fig. 3, SOS does not cancel mispointing, (i.e. the distance between the target BF position and the actual RA position), however it reduces the BLER degradation.

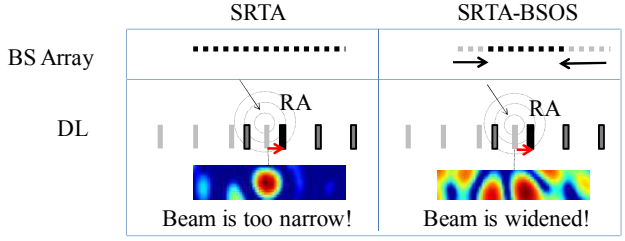

Fig. 3 SRTA and SRTA-BSOS systems

SOS is a closed loop mechanism. Initially, SRTA is run with $K_a = K$ antennas. The vehicle assesses the achieved SNR and compares it to a threshold (corresponding to 0.2 BLER). If the SNR is lower than the threshold, then, the vehicle sends a feedback message to the BS, the BS switches off half of its antennas ($K_a = K_a/2$) and updates A. Then, SRTA is run

again, with the new K_a and A parameters. K_a is divided by 2, successively, until the SNR threshold is exceeded. If the SNR increases over a threshold, then antennas are added so the beam is narrowed. The achieved SNR and energy saving are obtained by using (20), (21) with A instead of A_0:

$$x = \frac{\left|\sum_{k\in A} g_k(\vec{\alpha}+\rho(v)v^{-1}\vec{v})g_k^*(\vec{\alpha})\right|^2}{\left|\sum_{k\in A_0}|g_k(\vec{\alpha})|^2\right|^2} x_T, \quad (22)$$

$$e_S = |\sum_{k\in A}|g_k(\vec{\alpha})/g_0(\vec{\alpha})|^2|^2. \quad (23)$$

Here, e_S is lower than for SRTA when A is smaller than A_0.

Two variants of the scheme are investigated: 1) SRTA Random SOS, which reduces the number of utilized transmit antennas without giving any preference to specific antenna positions. 2) SRTA-Border SOS, which removes the antenna elements at the outer parts of the linear array from use in transmission, and thus reduces the array aperture.

D. SRTA with Polynomial Interpolation (SRTA-PI)

As illustrated by Fig. 4, SRTA-PI is based on SRTA, and mitigates mispointing by focusing "between" several "sensed" PAs positions instead of "over" a single position.

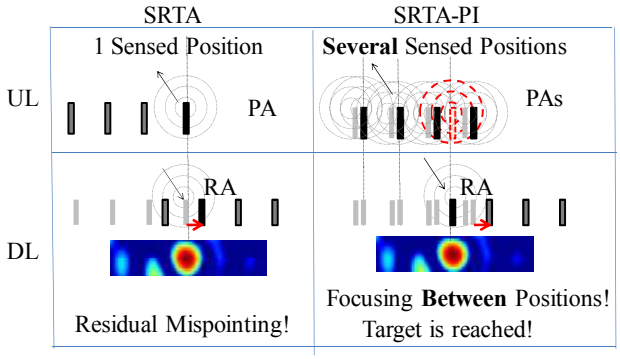

Fig. 4 SRTA-PI

Measurements are collected by multiple PAs, during multiple measurement periods to obtain a dense pattern of measurements in space, as illustrated in Fig. 5. Then, these measurements are used by a PI to compute the prediction.

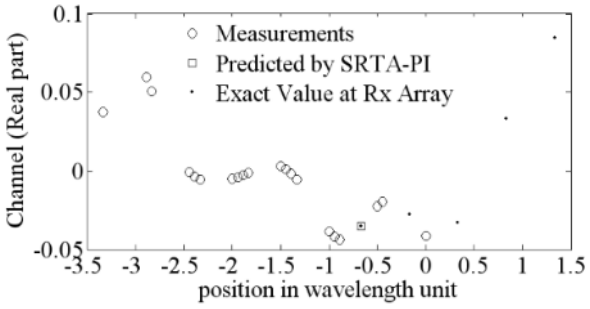

Fig. 5 SRTA-PI, one channel realization at 240kmph

To limit the PI complexity, only measurements collected during $t_a(v)$ seconds, every d seconds, and at least $t_a(v)$ seconds before BF are considered. More precisely, $K_a = K$, $A=A_0$, M, P, $L>1$. $\tau^{DL}=0.5\ \tau^{UL}=t_a(v)>t_0$. $t_a(v)$ and $r_a(v)$ are computed using (16),(17) to derive l_a as follows:

$$l_a = r_a(v) + 1 \quad (24)$$

The relations (17-19) are used to predict the RA position $\vec{\varepsilon}$. The reduced set of measurements C includes $\hat{g}_k\left(\overrightarrow{n_l^m}\right)$'s satisfying:

$$\delta^m = t' - \tau^m = t_a(v) + d.p, p \in \mathbb{N} \text{ and } \delta \leq 2t_a(v) \quad (25)$$

Let $n_l^m \in \mathbb{R}$ be the scalar coordinate along the vehicle short term linear trajectory, corresponding to $\overrightarrow{n_l^m}$. The BS stores n_l^m and $\hat{g}_k\left(\overrightarrow{n_l^m}\right)$ couples related to C, and performs PI over N_{meas} stored couples, with ε and $\gamma_k(\vec{\varepsilon})$ as the input and output of the PI operation, respectively. Hence, (24) is feasible for all $t' \in [0, \tau^{DL}[$, if τ^{UL} satisfies :

$$\tau^{UL} = 2\tau^{DL} = 2t_a(v). \quad (26)$$

The relation (24) guarantees that $\vec{\varepsilon}$ is between at least two n_l^m stored values, and avoids extrapolation, which is less reliable than interpolation. N_{meas} is given by:

$$N_{meas} = L\lceil t_a(v)d^{-1}\rceil \geq L. \quad (27)$$

PI is performed for the real and imaginary parts of the channel separately, with order $N_{meas} - 1$. PI complexity increases with N_{meas}. N_{meas} is large at low v, where SRTA is already sufficient [13]. We therefore trigger PI for v larger than a predefined threshold v_{PI}. For $v \leq v_{PI}$, SRTA is used instead. x and e_S are derived using equations (11),(12) using the prediction $\gamma_k(\vec{\varepsilon})$ obtained by PI.

IV. Initial Comparison Of Studied Schemes

TABLE I. Parameters and Expected Ordering

Parameter	RS	SRTA	SRTA BSOS/RSOS	SRTA-PI
τ^{DL}	$= t_0$	$= t_a(v) > t_0$		
δ^m	$= t_0$	$= t_a(v)$		$\in [t_a(v), 2t_a(v)]$
τ^{UL}/τ^{DL}	$= 1$			$= 2$
K_a	$= K$		$\leq K$	$= K$
L	=1	> 1		
l_a	=0	$= r_a(v)$		$= r_a(v) + 1$
P	=1			$= L$
M	=1			>1
N_{meas}	=1			$\geq L$
Best x	4	3	2	1
Best e_S	1	1	2	1
Most Simple	1	2	3	4

Table I gives an overview of the values of the parameters and an initial comparison, based on the mathematical expressions given in III, such as (11), (12), (14), (15), (20), (21). Regarding the prediction horizon δ^m, all SRTA schemes outperform RS by allowing higher values, thanks to the extended DL frame $t_a v$ (defined by (14)) which exceeds the RS fixed value t_0. Regarding energy efficiency, the two SOS schemes may use a lower number K_a of active antennas, and are then expected to save less energy than RS and SRTA schemes. Regarding the complexity, SRTA is more complex than RS, and SOS schemes are still more complex. SRTA-PI which performs PI of $N_{meas} > 1$ measurements collected for

multiple PAs ($P > 1$) at multiple times ($M > 1$) is probably the most complex. Regarding the robustness of SNR and BLER, RS should be the worst scheme. SRTA compensates PC speeds only, and should therefore be the 2nd best. SOS schemes enhance SRTA for NPC speeds, and should be the 3rd bests. Finally, SRTA-PI completely cancels mispointing and should hence be the best of all.

V. PERFORMANCE COMPARISON

A. Simulation assumptions and methodology

The following simulation assumptions are used: t_0= 2ms [14]; the carrier frequency f_0 is 2GHz; the wavelength is $\lambda = c/f_0$; where c=3.10^8 m/s is the speed of light; the BS has a linear array with K= 64 antennas separated by 0.5λ. In SRTA and SRTA-BSOS/RSOS the vehicle has L = 4 antennas separated by Δ, with $\Delta = 0.5\lambda$. For SRTA-PI, L= 5. The time step for frame extension is d= 1 ms, which is feasible in current standards [14]. It is also used for SRTA-PI measurements selection in (24). The vehicle speed v ranges from 0 to 300kmph. The target SNR is x_T=15.5 dB, which corresponds to a target BLER of 0.01 for 64QAM with code rate 3/4. v_{PI} =50 kmph is chosen to trigger PI, for SRTA-PI.

A large number of transmission situation events are generated by simulation. For each event, the angle of the BS antenna array and the angle of the vector $\vec{v}$ are generated randomly and are uniformly distributed between 0 and 2π. The position $\vec{\alpha}$ is also generated randomly. All other positions are deduced from $\vec{\alpha}$ and $\vec{v}$. Channel coefficients are then generated using a spatially correlated Ricean channel model with a LOS to total power ratio factor R which is either equal to 0 or 0.8. $R = 0$ corresponds to Non Line Off Sight (NLOS). For $R = 0.8$, the channel is dominated by the Line Of Sight (LOS) component. For each event, the following metrics are computed: the DL frame duration τ^{DL}, the selected RA index l_a, the number of active antennas K_a, the SNR, the BLER (using results stored in Table II based on link level simulations with Additive White Gaussian Noise) and the energy saving. These metrics are then averaged over events, and plotted as a function of speed v.

TABLE II. BLER FOR 64 QAM, RATE ¾, TURBO CODE, WITH BLOCK LENGTH OF 6000 BITS

SNR	14.5	15.0	15.5	15.7	16.0
BLER	1.0	0.8205	0.0125	0.0028	0.000001

B. Robustness and energy efficiency

In this sub-section, simulations use a pure NLOS channel.

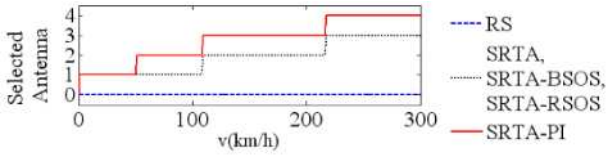

Fig. 6 Selected antennas

Fig. 6 illustrates l_a as a function of v. As discussed in Section IV, the SRTA and SRTA-RSOS/BSOS schemes share the same value. The RA is selected farther from the PA to compensate higher speeds. As explained in Section III-D, SRTA-PI uses a farther antenna to avoid extrapolation.

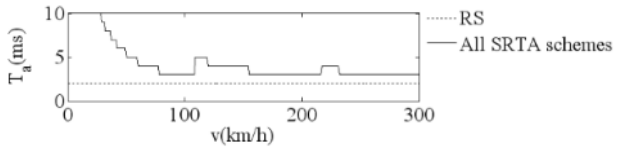

Fig. 7 Extended frame versus speed

Fig. 7 illustrates the DL frame duration $t_a(v)$ as a function of v. As explained in Section IV, all SRTA schemes use the same value, which decreases with speed but is always strictly higher than t_0, thus better than for RS.

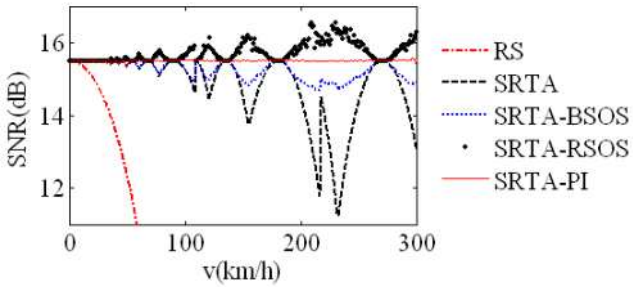

Fig. 8 SNR versus speed,

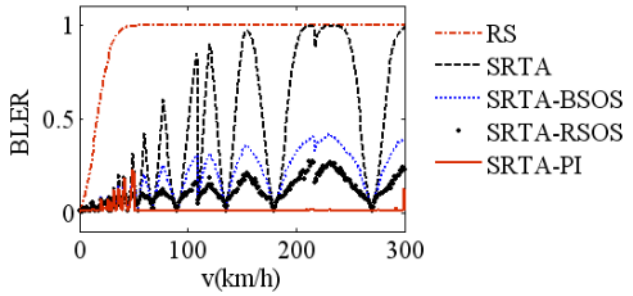

Fig. 9 BLER versus speed

Fig. 8 and 9 illustrate the SNR and the BLER versus v, respectively. With RS, the performance degrades strongly for speeds larger than 50 kmph, reaching a BLER of 1. Note in Table II that the BLER is a sensitive function of the attained SNR. As explained in Section III, SRTA compensates PC speeds but not NPC speeds. SRTA-BSOS/RSOS better handles NPC speeds by reducing SNR and BLER degradation. RSOS outperforms BSOS as Random switching creates a tapering [16] effect.

Fig. 10 and 11 illustrate the number of active transmit antennas K_a and the corresponding energy saving as a function of v, respectively. RS and SRTA use all antennas and achieve the maximum energy saving. For PC speeds, SRTA-BSOS/RSOS behave like SRTA, whereas for NPC speeds, $K_a < K$ antennas are used and less energy is saved. In other words, SOS schemes trade energy saving for BLER robustness.

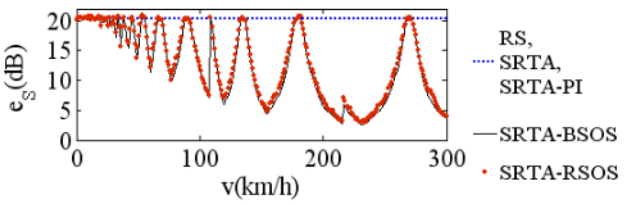

Fig. 10 Transmit Active Antennas versus speed

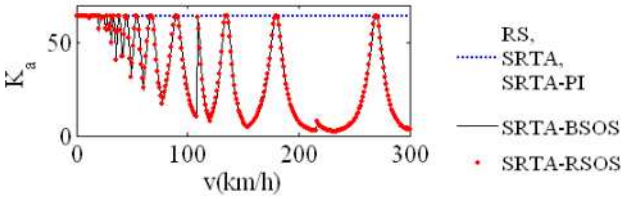

Fig. 11 Energy Saving versus speed

As illustrated by Fig. 8-11, SRTA-PI perfectly compensates all speeds larger than v_{PI}=50kmph, and still with maximum energy saving. For lower speeds, the PI is not triggered (as specified in III-D), as SRTA is sufficient. SRTA-PI therefore outperforms SRTA-RSOS w.r.t. energy saving and robustness.

Simulation results confirm the ordering identified in Section IV.

C. *Impact of Channel (LOS/NLOS)*

In this section simulations are run with R=0.8, i.e. with a dominating LOS component. Comparing Fig. 12 to Fig. 9 shows that the RS and SRTA schemes undergo a stronger mispointing effect in NLOS (Fig. 9) than in LOS (Fig.12). This is not surprising, as it has been shown that scattering increases spatial focusing of Time Reversal BF which is similar to MRT BF [17].

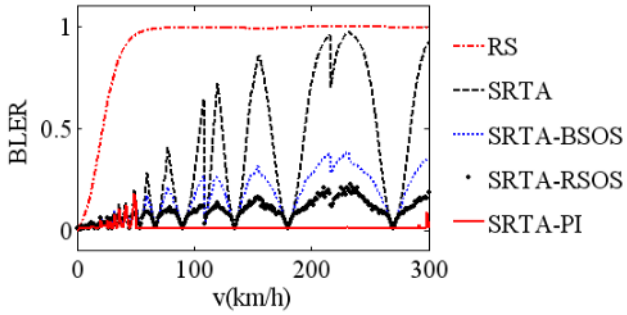

Fig. 12 BLER versus speed, strong LOS

VI. CONCLUSION

In this paper, we proposed three new schemes to improve the Separate Receive and Training Antenna technique to provide more robust energy efficient wireless downlink data transmission towards antennas upon very fast moving vehicles. The two first schemes, the "Border Switch Off Scheme" and the "Random Switch Off Scheme" simply switch off transmit antennas to widen the beam when beamforming mispointing is too severe. They slightly improve robustness by reducing energy savings. The third "Polynomial Interpolation" scheme is robust to all speeds up to 300 kmph and achieves maximum energy saving. This latter scheme relies on a Predictor Antennas Array and Polynomial Interpolation over multiple measurement samples. Ongoing next studies focus on reducing its complexity, while keeping its ability to perfectly control the block error rate at any speed.

ACKNOWLEDGMENT

This work has been performed in the framework of the FP7 project ICT-317669 METIS, which is partly funded by the EU.

REFERENCES

[1] Lo, T.K.Y., "Maximum ratio transmission," *Communications, IEEE Transactions on* , vol.47, no.10, pp.1458-1461, Oct 1999.

[2] Paulraj A, Nabar R, Gore D, "Introduction to Space-Time Wireless Communications", New York, USA, Cambridge University Press, 2008.

[3] Mohammed, S.K.; Chockalingam, A.; Sundar Rajan, B., "A Low-Complexity Precoder for Large Multiuser MISO Systems," *Vehicular Technology Conference, 2008. IEEE*, pp.797-801, 11-14 May 2008.

[4] Hong Yang; Marzetta, T.L., "Performance of Conjugate and Zero-Forcing Beamforming in Large-Scale Antenna Systems," *Selected Areas in Communications, IEEE Journal on*, vol.31, no.2, pp.172, Feb. 2013.

[5] Wagner, S.; Couillet, R.; Debbah, M.; Slock, D.T.M., "Large system analysis of linear precoding in correlated MISO broadcast channels under limited feedback," *IEEE transactions on information theory*, vol.58, no.7, pp.4509-4537, July 2012.

[6] Sui, Y.; Vihriala, J.; Papadogiannis, A.; Sternad, M.; Yang, W.; Svensson, T., "Moving cells: a promising solution to boost performance for vehicular users," *Communications Magazine, IEEE* , vol.51, no.6, pp., June 2013.

[7] Sternad, M.; Grieger, M.; Apelfröjd, R.; Svensson, T.; Aronsson, D.; Martinez, A.B., "Using "predictor antennas" for long-range prediction of fast fading for moving relays," *Wireless Communications and Networking Conference Workshops (WCNCW), 2012 IEEE* , v pp.253-257, April 2012.

[8] MSc thesis at TU Dresden by Ana Belén Martínez with the title "Using "Predictor Antennas" for Long-Range Prediction of Fast Fading for Moving Relays", Aug 20, 2012.

[9] Jamaly, A. Derneryd, T. Svensson, "Analysis of predictor antenna system for wireless moving relays", , Submitted Feb 2013.

[10] Grieger, M.; Fettweis, G., "Field trial results on uplink joint detection for moving relays," *Wireless and Mobile Computing, Networking and Communications (WiMob), 2012 IEEE 8th International Conference on* , vol., no., pp.586,592, 8-10 Oct. 2012.

[11] "Channel Prediction for Moving Relays", Ingrid Wiklund, August 2012, http://uu.diva-portal.org/smash/record.jsf?pid=diva2:607338, MSc thesis at Uppsala University.

[12] "Multiport Antenna Systems for Space-Time Wireless Communications" Nima Jamaly, PHD thesis ; Communication Systems Group Department of Signals and Systems Chalmers University of Technology, Gothenburg, Sweden 2013.

[13] D.T. Phan Huy, M. Hélard, "Large MISO Beamforming For High Speed Vehicles Using Separate Receive & Training Antennas", *IEEE International Symposium on Wireless Vehicular Communications , Dreden, 2-3 June 2013.*

[14] 3GPP; Technical Specification Group Radio Access Network; Evolved Universal Terrestrial Radio Access (E-UTRA), "Physical Channels and Modulation (Release 10)", TS 36.211, december 2012.

[15] W Zirwas, T. Giebel, H.Rohling, E. Schulz and J. Eichinger, "CSI-estimation for cooperative antennas," International OFDM Workshop, Hamburg, Germany, September 2003.

[16] C. Balanis, Antenna Theory: Analysis and Design, 2nd Ed, Wiley, 1997.

[17] A. Derode, A.Tourin, J.D. Rosny, M.Tanter, S.Yon, M.Fink "Taking Advantage of Multiple Scattering to Communicate with Time-Reversal Antennas" Physical Review Letters 2003, 90 (1), pp 014301-1-014301-4.